NEOPLASIA
www.neoplasia.com

Volume 13 Number 12 December 2011 pp. 1152–1161 1152

Noninvasive Imaging Reveals Inhibition of Ovarian Cancer by Targeting CXCL12-CXCR4[1,2]

Paramita Ray[*,3], Sarah A. Lewin[*,3], Laura Anne Mihalko[*], Bradley T. Schmidt[*], Kathryn E. Luker[*] and Gary D. Luker[*,†]

*Center for Molecular Imaging, Department of Radiology, University of Michigan Medical School, Ann Arbor, MI, USA; [†]Department of Microbiology and Immunology, University of Michigan Medical School, Ann Arbor, MI, USA

Abstract

Patients with metastatic ovarian cancer continue to have a dismal prognosis, emphasizing the need for new strategies to identify and develop new molecular targets for therapy. Chemokine CXCL12 and its receptor CXCR4 are upregulated in metastatic ovarian cancer cells and the intraperitoneal tumor microenvironment. CXCL12-CXCR4 signaling promotes multiple steps in proliferation and dissemination of ovarian cancer cells, suggesting that targeted inhibition of this pathway will limit tumor progression. To investigate CXCL12-CXCR4 signaling in ovarian cancer and establish effects of inhibiting this pathway on tumor progression and survival, we designed a *Gaussia* luciferase complementation imaging reporter system to detect CXCL12 binding to CXCR4 in ovarian cancer cells. In cell-based assays, we established that the complementation imaging reporter could detect CXCL12 binding to CXCR4 and quantify specific inhibition of ligand-receptor interaction. We monitored CXCL12-CXCR4 binding and inhibition in a mouse xenograft model of metastatic human ovarian cancer by imaging *Gaussia* luciferase complementation and assessed tumor progression with firefly luciferase. Bioluminescence imaging studies in living mice showed that treatment with AMD3100, a clinically approved inhibitor of CXCL12-CXCR4, blocked ligand-receptor binding and reduced growth of ovarian cancer cells. Treatment with AMD3100 also modestly improved overall survival of mice with metastatic ovarian cancer. The *Gaussia* luciferase complementation imaging reporter system will facilitate further preclinical development and optimization of CXCL12-CXCR4 targeted compounds for treatment of ovarian cancer. Our research supports clinical translation of existing CXCR4 inhibitors for molecular therapy for ovarian cancer.

Neoplasia (2011) 13, 1152–1161

Introduction

Ovarian cancer is the fifth leading cause of cancer death in women. Survival remains poor, with overall 5-year survival rates of ≈40% to 50% because patients with ovarian cancer typically are not diagnosed until malignant cells have metastasized throughout the peritoneal space into the abdomen and pelvis. Although up to 70% of patients respond initially to debulking surgery and chemotherapy with platinum- and taxane-based drugs, cancer recurs in most patients [1]. These facts underscore ongoing efforts to identify new therapeutic targets and strategies to improve treatment outcomes for patients with ovarian cancer [2–5].

Recent studies indicate that chemokine CXCL12 (also known as stromal-derived factor 1) and its receptor CXCR4 may drive progression of ovarian cancer, making these molecules highly promising targets for therapy [1,6]. Whereas normal ovaries express either no or minimally

Abbreviations: CXCL12-CG, chemokine CXCL12 fused to C-terminal fragment of *Gaussia* luciferase (CG); CG, secreted C-terminal fragment of *Gaussia* luciferase; NG-CXCR4, N-terminal fragment of *Gaussia* luciferase fused to chemokine receptor CXCR4

Address all correspondence to: Gary D. Luker, MD, Center for Molecular Imaging, University of Michigan Medical School, 109 Zina Pitcher Pl, A526 BSRB, Ann Arbor, MI 48109-2200. E-mail: gluker@umich.edu

[1]Research was supported by grants from the National Institutes of Health (R01CA136553, R01CA136829, and P50CA093990) and Department of Defense (W81XWH-09-1-0128).

[2]This article refers to supplementary materials, which are designated by Figures W1 to W3 and are available online at www.neoplasia.com.

[3]These authors contributed equally to the work.

Received 29 July 2011; Revised 3 November 2011; Accepted 8 November 2011

DOI 10.1593/neo.111076

detectable CXCR4, this receptor is expressed by ovarian cancer cells in ≈60% of patients [7]. Expression of CXCR4 on ovarian cancer cells is an independent prognostic factor for worse progression-free and overall survival relative to patients without detectable CXCR4 on malignant cells [7]. CXCL12 is expressed by more than 90% of ovarian cancer cells and carcinoma-associated mesothelial cells, resulting in elevated levels of this chemokine in ascites of patients with ovarian cancer [8–10]. CXCL12 signaling through CXCR4 activates pathways that enhance proliferation, migration, and invasion of ovarian cancer cells [8,11,12]. CXCL12-CXCR4 signaling also increases tumor angiogenesis through effects on endothelial cells and recruitment of circulating endothelial progenitor cells [13–15]. Collectively, signaling pathways mediated by CXCL12-CXCR4 activate multiple processes that contribute to growth and metastasis of ovarian cancer cells.

A key challenge in successfully targeting CXCL12-CXCR4 and other molecules in ovarian cancer is determining the pharmacodynamics of a compound in the tumor microenvironment. Even in preclinical models, effects of a chemotherapeutic agent on a specific molecule or pathway typically are inferred by studies of surrogate tissues, such as blood cells, or histologic analysis of excised tumors at single time points. These methods preclude longitudinal studies of molecular targeting of a compound in a tumor and resultant effects on disease progression in the same animal. As a result, it is difficult to directly link pharmacodynamics of a therapeutic agent in a tumor microenvironment to reduced tumor growth *in vivo*.

Our laboratory has developed imaging reporters to quantify activation of chemokine receptors in cell-based assays and living mice [16,17]. We recently devised an imaging system based on *Gaussia* luciferase protein fragment complementation to quantify ligand-receptor binding, the initial step in chemokine receptor signaling [18]. We used this optical imaging technology to show that intercellular binding between CXCL12 and CXCR4 occurs in a mouse model of disseminated intraperitoneal ovarian cancer. We also established that treatment with AMD3100, a clinically approved inhibitor of CXCL12-CXCR4, blocked ligand-receptor binding in the tumor microenvironment of mice with disseminated ovarian cancer. Furthermore, using separate imaging reporters to monitor CXCL12-CXCR4 binding and tumor growth, we demonstrated that single-agent therapy with AMD3100 blocked CXCL12-CXCR4 binding, reduced tumor growth, and modestly prolonged survival of mice with disseminated ovarian cancer. These results establish an *in vivo* imaging technology for pharmacodynamics of CXCL12-CXCR4 inhibitors in preclinical drug development and support clinical translation of compounds targeting this chemokine receptor for treatment of women with ovarian cancer.

Materials and Methods

Cells

HeyA8 ovarian cancer cells (provided by Gordon Mills, MD Anderson Cancer Center) were stably transduced with recombinant lentiviruses for CXCL12 fused to the C-terminal fragment of *Gaussia* luciferase (CXCL12-CG) or the N-terminal fragment of *Gaussia* luciferase fused to CXCR4 (NG-CXCR4). We transduced HeyA8 cells with a secreted C-terminal fragment of *Gaussia* luciferase (CG). NG-CXCR4 cells also were transduced with firefly luciferase [19]. Batch populations of cells were used for all experiments. Cells were cultured in Dulbecco modified Eagle medium (Invitrogen, Carlsbad, CA), 10% fetal bovine serum, 1% glutamine, and 0.1% penicillin/streptomycin/gentamicin. Cells were grown in a 37°C incubator with 5% CO_2.

Reverse Transcription–Polymerase Chain Reaction and Quantitative Reverse Transcription–Polymerase Chain Reaction

RNA was extracted from cells using TRIzol reagent according to the manufacturer's directions. Expression of CXCL12-α in HeyA8 cells was determined by reverse transcription–polymerase chain reaction (RT-PCR) using primers 5′-TGAGCAGTGAATGATTCAGTGTT-3′ and 5′-CTTCTCCTGGACCATTTTCACAT-3′. Messenger RNA for CXCL12-CG or CG in stably transduced HeyA8 cells was quantified using primers for CG: 5′-GGCGATCGTCGACATTCCTG-3′ and 5′-GTCACCACCGGCCCCCTTG-3′. Primers for glyceraldehyde phosphate dehydrogenase were 5′-GAAGGTGAAGGTCGGAGT-3′ and 5′-GAAGATGGTGATGGGATTTC-3′. Samples for quantitative RT-PCR were analyzed on an Eppendorf RealPlex QRT-PCR instrument using SYBR Green detection. Amounts of messenger RNA for CXCL12-CG and CG were normalized to glyceraldehyde phosphate dehydrogenase and expressed as $\Delta\Delta C_t$ values.

Flow Cytometry

Cells were stained with an antibody to CXCR4 (clone 12G5; R&D Systems, Minneapolis, MN) or matched isotype control as described previously [20].

Western Blot Analysis

Cells were cultured in serum-free medium overnight and then stimulated for 10 minutes with various concentrations of recombinant CXCL12-α (R&D Systems). Cell lysates were blotted for phosphorylated AKT (Cell Signaling, Danvers, MA) as described previously [21]. Blots were stripped and reprobed for total AKT as a loading control.

Coculture Experiments

NG-CXCR4 cells were coseeded with either CXCL12-CG or CG cells in black-walled 96-well plates (1×10^4 cells of each type). Cells were plated in standard culture medium and then switched the following day to phenol red–free Dulbecco modified Eagle medium (Invitrogen) without serum for assays. In selected experiments, cells were incubated with AMD3100 to inhibit CXCL12 binding to CXCR4 (Tocris, Ellisville, MO), small molecule inhibitors of CXCR7 (gift of ChemoCentryx, Mountain View, CA), or vehicle control for AMD3100 (phosphate-buffered saline [PBS]) at concentrations listed in figure legends. Bioluminescence from *Gaussia* luciferase complementation was measured as described previously and normalized to total protein per well quantified by sulforhodamine B staining [21].

Animal Studies

All animal procedures were approved by the University of Michigan Committee for the Use and Care of Animals. A total of 1.25 to 2.5×10^5 NG-CXCR4 cells were injected with an equal number of CXCL12-CG or CG cells intraperitoneally in 100 μl of 0.9% NaCl into 5- to 7-week-old female $Ncr^{Nu/Nu}$ (Harlan, Indianapolis, IN) or NOD/SCID $IL2r\gamma^{-/-}$ female mice (Taconic, Hudson, NY) [22]. To inhibit CXCL12 binding to CXCR4, we treated mice with AMD3100 administered either as 1.25 mg/kg i.p. injections twice per day or as 14-day 0.5-μl/h osmotic pumps (Alzet, Cupertino, CA) loaded with 25 mg/ml AMD3100. Control mice received injections or pumps with 0.9% NaCl. Pumps were implanted 10 days after injection of ovarian cancer cells.

Animal Imaging Studies

Bioluminescence imaging was performed on an IVIS Spectrum (Caliper, Hopkinton, MA). For *Gaussia* luciferase imaging, mice were injected intravenously through tail vein with 4 mg/kg coelenterazine [23]. Mice were imaged immediately after injection using 3-minute acquisition and large binning. Firefly luciferase imaging was performed as described previously [24]. Data were quantified as photon flux with Living Image software (Caliper) to account for differences in image acquisition time for firefly luciferase imaging.

Statistics

Graphs and statistical analyses were prepared with GraphPad Prism (GraphPad Software, La Jolla, CA). Cell culture studies were performed three to five times, whereas animal studies were performed two to three times. Data were plotted as mean values with SEM. Pairs of data were analyzed by Mann-Whitney *U* test to determine statistically significant differences. Kaplan-Meier survival curves were analyzed by Gehan-Breslow-Wilcoxon test.

Results

HeyA8 Cells Activate CXCL12-CXCR4 Signaling

Chemokine receptor CXCR4 is expressed by several ovarian cancer cell lines and approximately 60% of metastatic human ovarian cancers [8,25]. We used flow cytometry to analyze cell surface expression of CXCR4 on HeyA8 ovarian cancer cells. These cells express modest levels of CXCR4 (Figure 1*A*). HeyA8 cells also activate AKT, a known downstream effector of CXCR4 signaling, in response to CXCL12 (Figure 1*B*). HeyA8 cells do not express detectable CXCL12 as determined by RT-PCR. These results establish that HeyA8 ovarian cancer cells have intact CXCL12-CXCR4 signaling, validating them as an appropriate model for imaging studies of CXCL12-CXCR4 binding and function.

Gaussia *Luciferase Complementation Detects CXCL12-CXCR4 Binding in Cell-Based Assays*

We recently described a protein fragment complementation system using *Gaussia* luciferase to quantify chemokine binding to target receptors [18]. In this system, N- and C-terminal fragments of *Gaussia* luciferase are fused to the extracellular N-terminus of CXCR4 and the C-terminus of CXCL12 (NG-CXCR4 and CXCL12-CG, respectively; Figure 2*A*). These orientations of fusion proteins maximize bioluminescence from CXCL12 binding to CXCR4 [18]. Binding of CXCL12-CG to NG-CXCR4 brings together luciferase fragments to produce light as a quantitative measure of ligand-receptor binding. Because *Gaussia* luciferase complementation is fully reversible, dissociation of CXCL12 from CXCR4 turns off bioluminescence [26]. NG and CG fragments are positioned to detect ligand binding in the extracellular space and in intracellular compartments, using advantages of *Gaussia* luciferase as an ATP-independent enzyme with broad pH optimum [23].

We transduced HeyA8 cells with lentiviral vectors to generate stable populations of cells secreting CXCL12-CG or expressing NG-CXCR4, respectively. As a control for bioluminescence from nonspecific association of NG and CG fragments alone, we also established populations of cells that secrete an unfused CG fragment. HeyA8-NG-CXCR4 cells expressed modestly higher levels of CXCR4 on the cell surface than parental HeyA8 cells (Figure 2*B*). HeyA8-CXCL12-CG and HeyA8-CG cells expressed comparable levels of CG by QRT-PCR (data not shown).

To establish that *Gaussia* luciferase complementation could quantify intercellular CXCL12-CXCR4 binding in ovarian cancer cells, we co-cultured HeyA8-NG-CXCR4 cells with equal numbers of HeyA8 cells secreting either CXCL12-CG or CG. After 2 hours of coculture, bioluminescence from CXCL12-CG binding to NG-CXCR4 was about eight-fold greater than nonspecific association of secreted CG with NG-CXCR4 ($P < .01$; Figure 2*C*). We also measured changes in bioluminescence over time in this coculture model. Bioluminescence from CXCL12-CG binding to NG-CXCR4 was significantly greater than control signal (CG and NG-CXCR4) within 15 minutes ($P < .01$; Figure 2*D*). Signal from CXCL12-CG and NG-CXCR4 cocultures increased over time, whereas minimal light from CG and NG-CXCR4 did not change for 2 hours. Collectively, these data demonstrate that *Gaussia* luciferase complementation can detect CXCL12-CXCR4 binding in ovarian cancer cells.

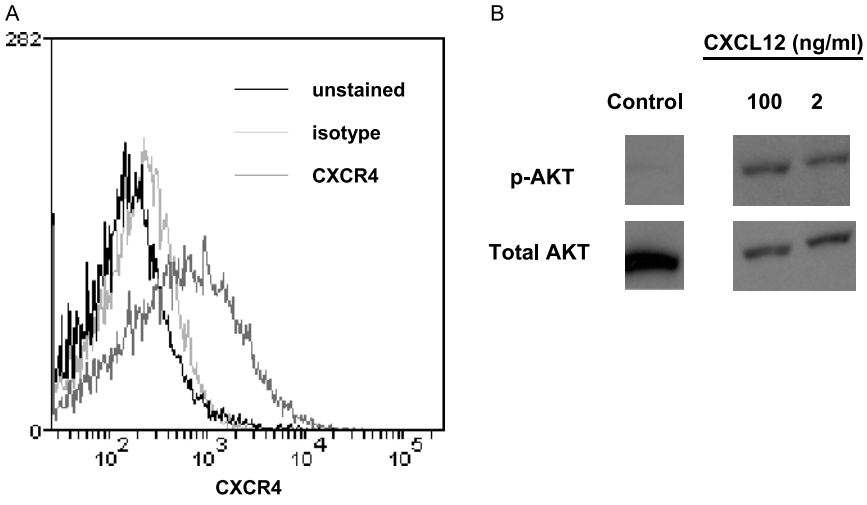

Figure 1. HeyA8 ovarian cancer cells express functional CXCR4. (A) Cell surface levels of CXCR4 on HeyA8 cells were determined by flow cytometry. Dark line indicates unstained; light line, isotype antibody control; and intermediate line, CXCR4 antibody. (B) HeyA8 cells were serum starved overnight and then incubated with 2 or 100 ng/ml CXCL12 for 10 minutes. Cell lysates were probed for phosphorylated AKT (p-AKT, active form) and total AKT as a control for protein loading.

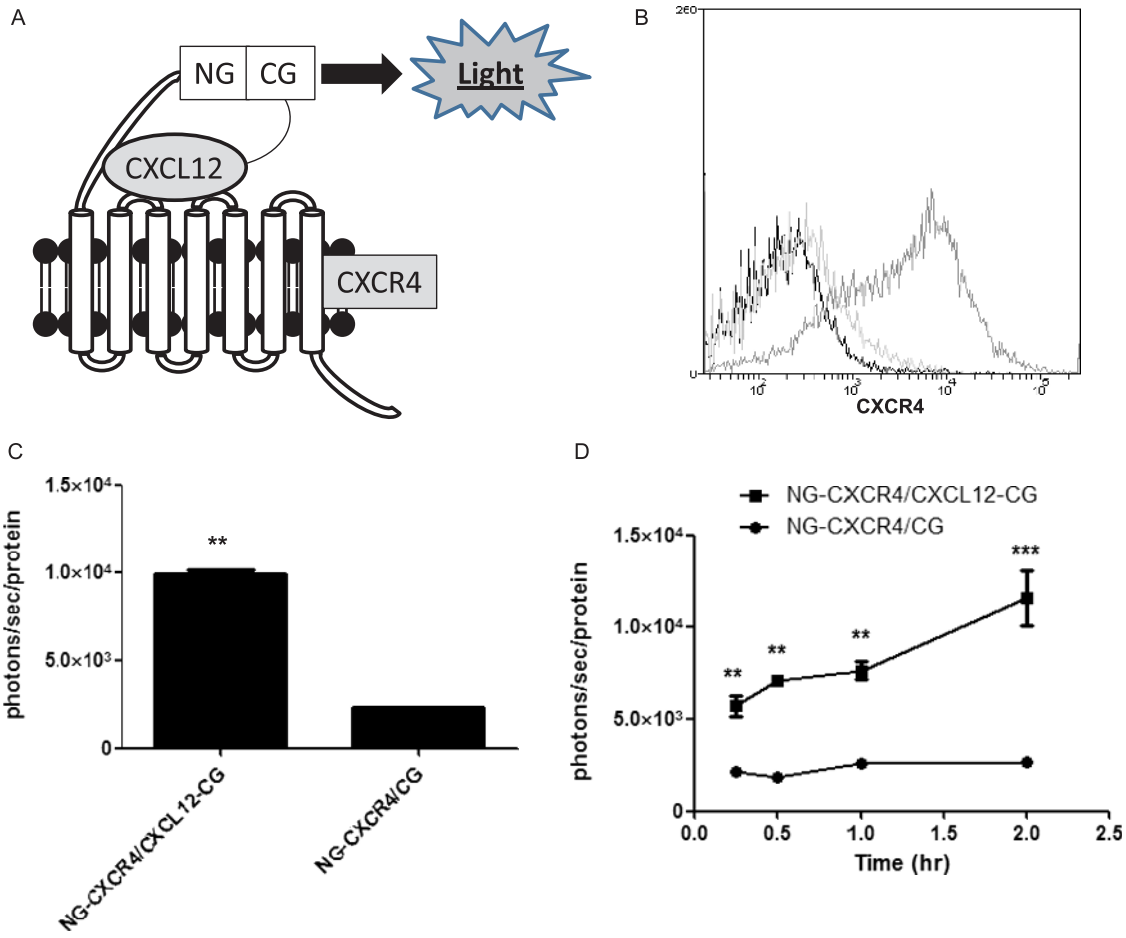

Figure 2. *Gaussia* luciferase complementation detects CXCL12-CXCR4 binding in cell-based assays. (A) Schematic diagram of complementation system. The C-terminus of CXCL12 is fused to the C-terminal fragment of *Gaussia* luciferase (CXCL12-CG), and the N-terminal fragment of *Gaussia* is fused to the extracellular N-terminus of CXCR4 (NG-CXCR4). These orientations of fusion proteins position NG and CG fragments in the extracellular space. CXCL12 binding to CXCR4 brings together NG and CG enzyme fragments, reconstituting an active enzyme to produce light. (B) Flow cytometry shows expression of CXCR4 on the surface of NG-CXCR4 cells. Dark line indicates unstained; light line, isotype antibody control; and intermediate line, CXCR4 antibody. (C) HeyA8-NG-CXCR4 cells were cocultured with equal numbers of HeyA8-CXCL12-CG (CXCL12-CG/NG-CXCR4) or control cells secreting unfused CG (CG/NG-CXCR4) for 2 hours before quantifying *Gaussia* luciferase bioluminescence. Photon flux was normalized to relative amounts of total protein per well, and data were expressed as mean values ± SEM for each coculture ($n = 4$ per condition). (D) Cocultures of HeyA8-CXCL12-CG/NG-CXCR4 or HeyA8-CG/NG-CXCR4 cells were incubated for various periods through 2 hours before quantifying Gaussia luciferase bioluminescence as described in C ($n = 4$ per condition). $^{**}P < .01$. $^{***}P < .005$.

AMD3100 Blocks CXCL12-CXCR4 Complementation in Intact Cells

To quantify inhibition of CXCL12 binding to CXCR4, we treated cells with AMD3100, a clinically approved inhibitor of CXCL12-CXCR4 [27]. We prepared cocultures of HeyA8 NG-CXCR4 cells with equal numbers of HeyA8-CXCL12-CG or HeyA8-CG cells. After allowing cells to adhere overnight, we changed cells to medium containing 1 μM AMD3100 for various periods through 4 hours. As a control, we incubated cells with 1 μM CCX771, a specific inhibitor of CXCL12 binding to CXCR7 [28]. Bioluminescence from CXCL12-CG binding to NG-CXCR4 decreased within 30 minutes of treatment with AMD3100 ($P < .01$; Figure 3*A*). Signal decreased progressively over time to ≈50% of initial bioluminescence by 4 hours ($P < .01$). By comparison, AMD3100 did not alter background signal from secreted CG and NG-CXCR4, and incubation with CCX771 had no effect on bioluminescence produced by CXCL12-CG/NG-CXCR4 or the control pair of CG/NG-CXCR4. Treatment with 1 μM AMD3100 also decreased bioluminescence from CXCL12-CG binding to NG-CXCR4 relative to cocultures of these cells treated with PBS vehicle control (Figure W1).

Treatment with AMD3100 for 2 hours also produced dose-dependent inhibition of complementation between CXCL12-CG and NG-CXCR4 (Figure 3*B*). We observed a significant decrease in bioluminescence with 10 nM AMD3100, and maximum inhibition occurred with 100 nM of this drug ($P < .05$ and $P < .01$, respectively). The EC_{50} for inhibiting bioluminescence from CXCL12-CG binding to NG-CXCR4 was ≈30 nM AMD3100, which is comparable to the ≈20 nM EC_{50} value reported previously for inhibiting binding of recombinant CXCL12 to CXCR4 at 4°C [29]. The CXCR7 inhibitor CCX771 did not affect bioluminescence from CXCL12-CG and NG-CXCR4. Neither AMD3100 nor CCX771 changed the low-level signal from secreted CG and NG-CXCR4.

We also tested to what extent AMD3100 inhibits a preexisting complementation signal from CXCL12-CG binding to NG-CXCR4,

which more closely models use of AMD3100 to treat ovarian cancer. We incubated cocultures of HeyA8-CXCL12-CG/HeyA8-NG-CXCR4 cells and HeyA8-CG/NG-CXCR4 cells for 4 hours and then added increasing concentrations of AMD3100 for an additional 4 hours. Under these conditions, we again observed a significant decrease in bioluminescence from 10 nM AMD3100, although the EC_{50} for inhibiting established ligand-receptor binding increased to ≈200 nM ($P < .05$; Figure 3*C*). The increase in EC_{50} likely is due to the inability of AMD3100 to disrupt CXCL12-CXCR4 complexes that formed and internalized before adding drug.

Imaging CXCL12-CXCR4 Complementation in a Mouse Model of Ovarian Cancer

To image CXCL12 binding to CXCR4 *in vivo*, we injected HeyA8-NG-CXCR4 cells with either HeyA8-CXCL12-CG or HeyA8-CG cells intraperitoneally into nude mice. This model reproduces intraperitoneal metastasis of ovarian cancer, which is the principal site of disease in patients. HeyA8-NG-CXCR4 cells also stably expressed firefly luciferase, an enzyme that uses a different substrate than *Gaussia* luciferase. Bioluminescence imaging for firefly luciferase provides a noninvasive measure of relative numbers of these cells in the peritoneal cavity independent of *Gaussia* luciferase complementation.

Gaussia luciferase imaging in mice injected with HeyA8-CXCL12-CG and HeyA8-NG-CXCR4 cells showed bioluminescence from CXCL12 binding to CXCR4 in multiple sites throughout the abdomen (Figure 4*A*). Signal from CXCL12-CG and NG-CXCR4 was ≈15-fold greater than the control pair of CG and NG-CXCR4, the latter of which was nearly at background levels ($P < .01$; Figure 4*B*). Firefly luciferase imaging revealed diffuse signal from HeyA8-NG-CXCR4 cells in both groups of mice, establishing that disseminated disease had developed in both cohorts of animals. After mice were killed, we observed multiple tumor masses disseminated throughout the abdomen (data not shown). In these and other *in vivo* images, we note that bioluminescence from *Gaussia* luciferase does not strictly coincide with firefly luciferase. Such differences likely result from relatively greater attenuation of signal from *Gaussia* luciferase, which emits light at 480 nm as compared with peak emission of firefly luciferase at 560 nm. In addition, *Gaussia* luciferase bioluminescence only is produced at sites where CXCL12-CG binds to NG-CXCR4, whereas NG-CXCR4 cells constitutively express firefly luciferase independent of binding to CXCL12-CG.

To validate the complementation system for quantifying inhibition of CXCL12-CXCR4 binding *in vivo*, we injected HeyA8-CXCL12-CG and HeyA8-NG-CXCR4 intraperitoneally in mice. After obtaining baseline imaging for *Gaussia* luciferase complementation, we treated groups of animals with AMD3100 or vehicle control for 3 days and then repeated the imaging study. Mice treated with AMD3100 had bioluminescence only slightly above baseline, which was similar to the minimal signal produced by nonspecific association of CG and

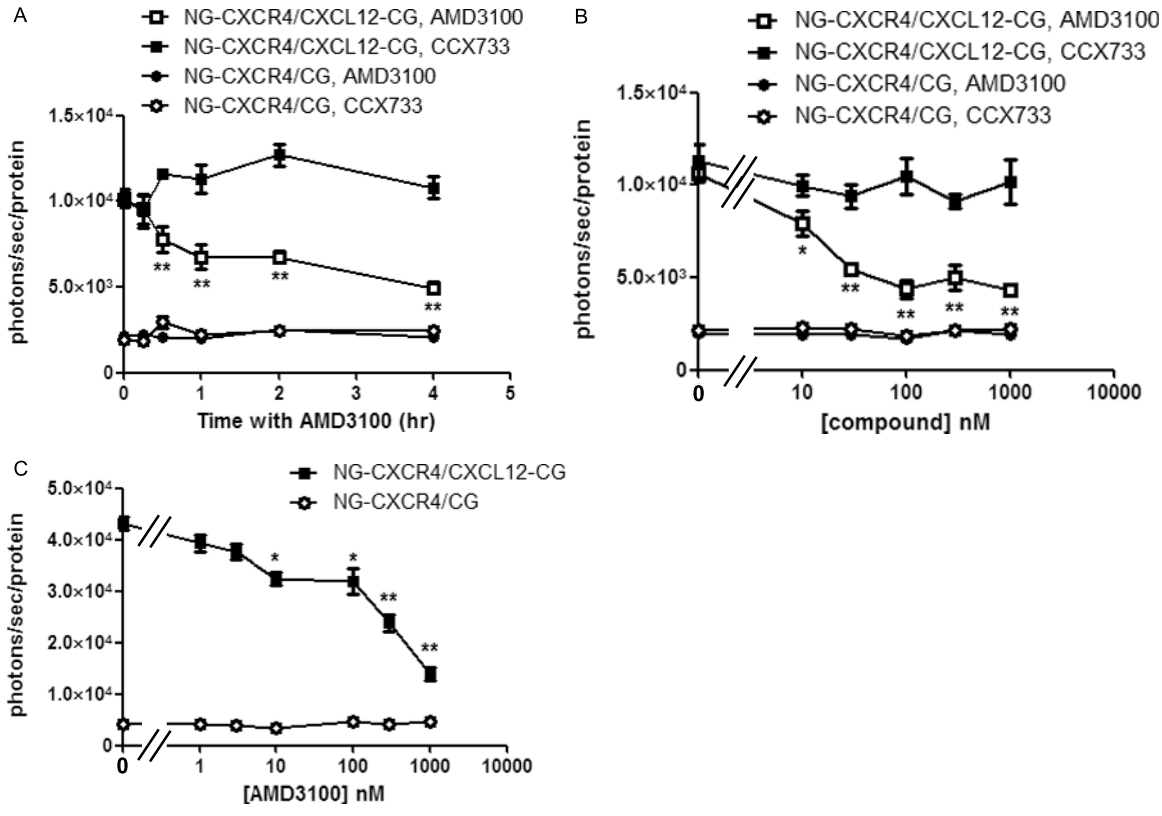

Figure 3. AMD3100 inhibits bioluminescence from CXCL12-CXCR4 binding. (A) Cocultures of HeyA8 cells (CXCL12-CG/NG-CXCR4 or CG/NG-CXCR4) were incubated for increasing periods with 1 μM AMD3100, a CXCR4 inhibitor, or CCX771, an inhibitor of CXCL12 binding to CXCR7. *Gaussia* luciferase bioluminescence was quantified as described in Figure 2, and data were presented as mean values ± SEM ($n = 4$ per condition). (B) Cocultures of CXCL12-CG/NG-CXCR4 or control CG/NG-CXCR4 cells were incubated for 2 hours with increasing concentrations of AMD3100 or CCX771, respectively, before measuring bioluminescence from *Gaussia* luciferase ($n = 4$ per condition). (C) Pairs of HeyA8 cells were incubated for 4 hours before adding increasing concentrations of AMD3100 for an additional 4 hours before quantify bioluminescence ($n = 4$ per condition). *$P < .05$. **$P < .01$.

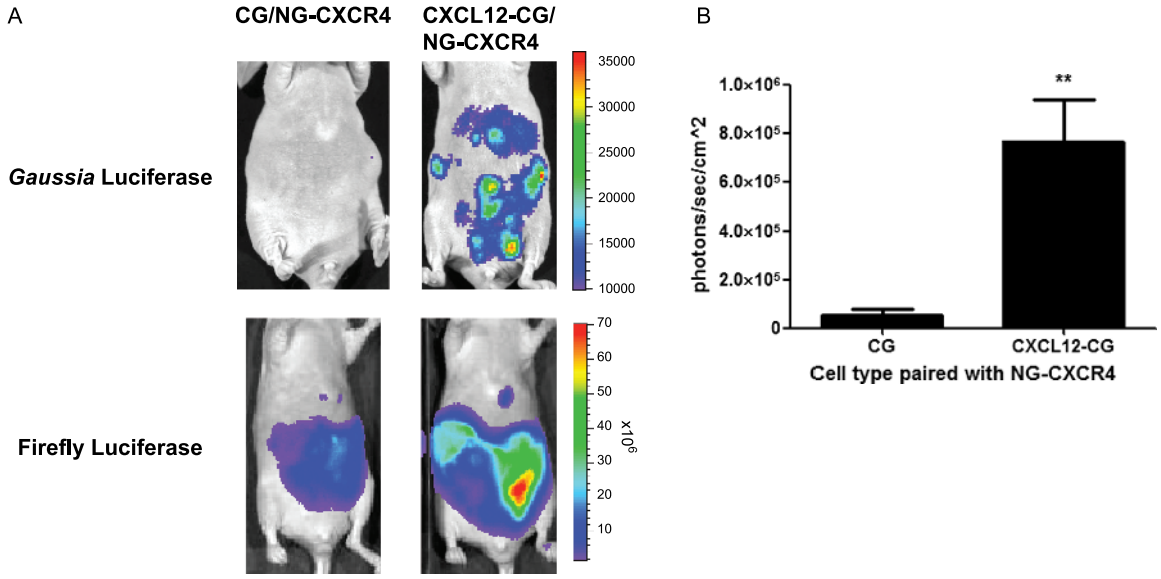

Figure 4. Imaging CXCL12-CXCR4 binding in living mice with disseminated intraperitoneal ovarian cancer. (A) Pairs of HeyA8 ovarian cancer cells (CG/NG-CXCR4) or (CXCL12-CG/NG-CXCR4) were injected intraperitoneally into mice (1.25×10^5 of each cell type per mouse). Two weeks after injection, mice were imaged with coelenterazine to detect bioluminescence from *Gaussia* luciferase complementation in cells with the interacting pair (CXCL12-CG/NG-CXCR4) or the control pair (CG/NG-CXCR4). Firefly luciferase images show relative numbers of HeyA8-NG-CXCR4 cells, which constitutively express this imaging reporter. Scale bars for imaging data depict ranges of pseudocolors with red and blue representing highest and lowest photon flux values, respectively. (B) Quantified data for *Gaussia* luciferase bioluminescence ($n = 5$ per group). Data were graphed as mean values ± SEM. $^*P < .05$.

NG-CXCR4 (Figure 5*A*; see Figure 4*A*). Treatment with AMD3100 reduced bioluminescence from CXCL12-CG binding to NG-CXCR4 below the pretreatment value, whereas continued tumor growth caused *Gaussia* luciferase bioluminescence signal to increase in animals receiving vehicle control ($P < .05$; Figure 5*B*). By comparison, bioluminescence from firefly luciferase increased in both groups of mice due to tumor growth during 3 days (Figure 5, *C* and *D*). The increase in firefly luciferase signal was slightly greater in mice treated with vehicle control, although differences between groups were not significant at this time point. Because AMD3100 suppressed *Gaussia* luciferase complementation below pretreatment levels while firefly luciferase signal increased, these data indicate that loss of *Gaussia* bioluminescence is due to inhibition of CXCL12 binding to CXCR4 rather than general cell death.

Noninvasive Imaging of CXCR4-Targeted Therapy in Living Mice

Having established the ability to noninvasively quantify CXCL12-CXCR4 binding *in vivo*, we used this imaging system to monitor response to targeted therapy. We injected 1.25×10^5 cells each of HeyA8-CXCL12-CG and HeyA8-NG-CXCR4 cells intraperitoneally to generate disseminated ovarian cancer. After allowing tumors to grow for 10 days, we treated mice with either AMD3100 or vehicle control. Because AMD3100 has a short (3-4 hours) serum half-life, we delivered this drug or vehicle control through subcutaneous osmotic pumps to maintain effective levels of compound during prolonged periods of treatment. Bioluminescence imaging for *Gaussia* luciferase after 5 and 11 days of treatment showed significantly lower signal in mice treated with AMD3100 compared with vehicle control ($P < .05$ and $P < .01$, respectively; Figures 6*A* and W2). These imaging data established that AMD3100 effectively inhibited CXCL12 binding to CXCR4 over the course of treatment. We imaged firefly luciferase activity from HeyA8-NG-CXCR4 cells to determine effects of treatment on tumor growth. Mice treated with AMD3100 had significantly lower firefly luciferase signal on days 5 and 11 of therapy, showing that this compound limited growth of ovarian cancer cells *in vivo* (Figure 6, *B* and *C*). *Gaussia* luciferase complementation between CXCL12-CG and NG-CXCR4 also could be blocked by AMD3100 in HeyA8-CXCL12-CG/HeyA8-NG-CXCR4 cells recovered from ascites, indicating that cells did not become resistant during the period of therapy (Figure W3). Furthermore, treatment with AMD3100 modestly extended overall survival of mice relative to animals receiving vehicle control (Figure 6*D*; $P < .05$). Using bioluminescence imaging to monitor pharmacodynamics and effects of therapy, these data establish that targeted inhibition of CXCL12-CXCR4 reduces tumor growth and modestly increases survival of mice with ovarian cancer.

Discussion

Prognosis in ovarian cancer remains dismal because most patients present with advanced disease with malignant cells disseminated throughout the peritoneal space. To improve outcomes for these patients, there is an unmet clinical need for new therapeutic strategies to limit growth of ovarian cancer. Chemokine CXCL12 and its receptor CXCR4 seem to be promising therapeutic targets in ovarian cancer. CXCL12-CXCR4 signaling is proposed to regulate metastasis of more than 20 different cancers, including intraperitoneal dissemination of gastric cancer [30]. The expression of CXCR4 in ovarian cancer and levels of CXCL12 in ascites both increase progressively with higher stages of disease, suggesting that CXCL12-CXCR4 signaling may contribute to tumor growth and dissemination [25,31]. Association of CXCL12-CXCR4 with metastatic ovarian cancer is further strengthened by studies showing that the tumor microenvironment upregulates this receptor, promoting proliferation and invasion of ovarian cancer cells through the extracellular

matrix [10,25,31]. Blocking CXCL12-CXCR4 signaling may limit progression of ovarian cancer and provide a new therapeutic strategy to prevent or more effectively treat advanced stage disease.

We used a new optical imaging reporter system based on *Gaussia* luciferase complementation to quantify CXCL12 binding to CXCR4 in the microenvironment of ovarian cancer. We previously demonstrated that this complementation system could image CXCL12-CXCR4 binding in breast cancer cells that lack expression of endogenous CXCR4 [18]. In the current study, we established that this imaging system also generates robust signal using HeyA8 cells that normally express wild-type unfused CXCR4. Wild-type CXCR4 will bind CXCL12-CG without generating light, serving as a competitor for complementation between CXCL12-CG and NG-CXCR4. The ability to use *Gaussia* luciferase complementation to quantify CXCL12-CXCR4 binding in cells with endogenous CXCR4 extends applications of this imaging system to the large number of ovarian and other cancer cells that express this receptor. Because *Gaussia* and firefly luciferases use different substrates, we also were able to combine *Gaussia* luciferase imaging for CXCL12-CXCR4 binding with firefly luciferase imaging for tumor growth *in vivo*. Using this system, we established that treatment with AMD3100, a clinically approved inhibitor of CXCL12 binding to CXCR4, blocked this ligand-receptor pair in cell-based assays and living mice with disseminated ovarian cancer. Inhibiting CXCL12 binding to CXCR4 decreased growth of ovarian cancer cells and modestly prolonged survival of mice relative to animals treated with vehicle control. Collectively, these data suggest that

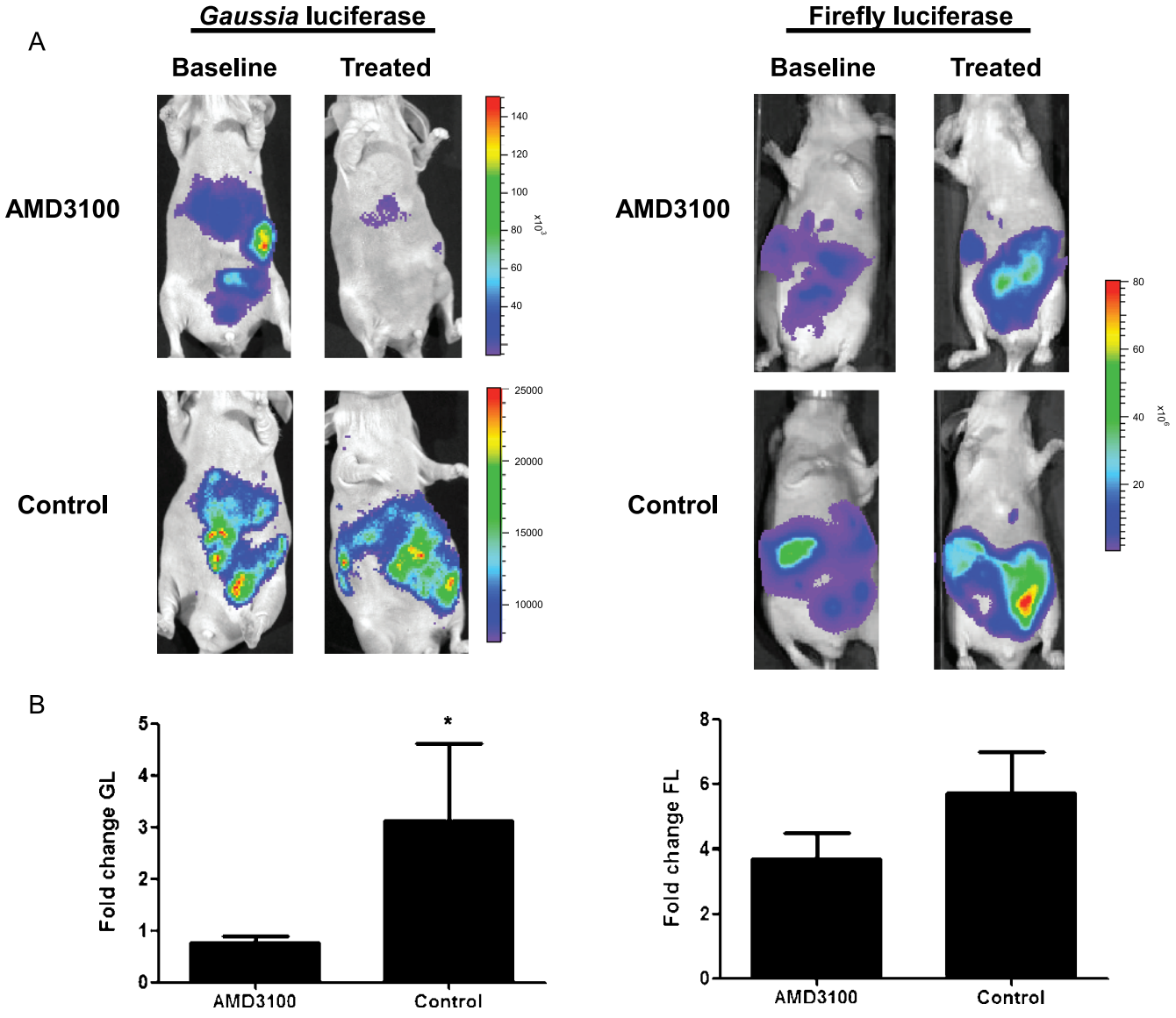

Figure 5. AMD3100 blocks CXCL12-CXCR4 binding *in vivo*. (A) Mice were injected intraperitoneally with 2.5×10^5 each of HeyA8-CXCL12-CG and NG-CXCR4 cells. Baseline images for *Gaussia* luciferase complementation and firefly luciferase expressed constitutively by NG-CXCR4 cells were obtained 7 days after injecting ovarian cancer cells. Mice then were treated for 3 days with AMD3100 or vehicle control before repeating imaging studies. Representative images for mice treated with AMD3100 or vehicle control are displayed. Scale bars denote pseudocolor displays for bioluminescence for *Gaussia* and firefly luciferase images, respectively. (B) Quantified data for *Gaussia* luciferase (GL) activity (n = 7-8 per group). Change in bioluminescence from posttreatment to pretreatment values was calculated for each mouse, and mean values ± SEM were presented. *$P < .05$.

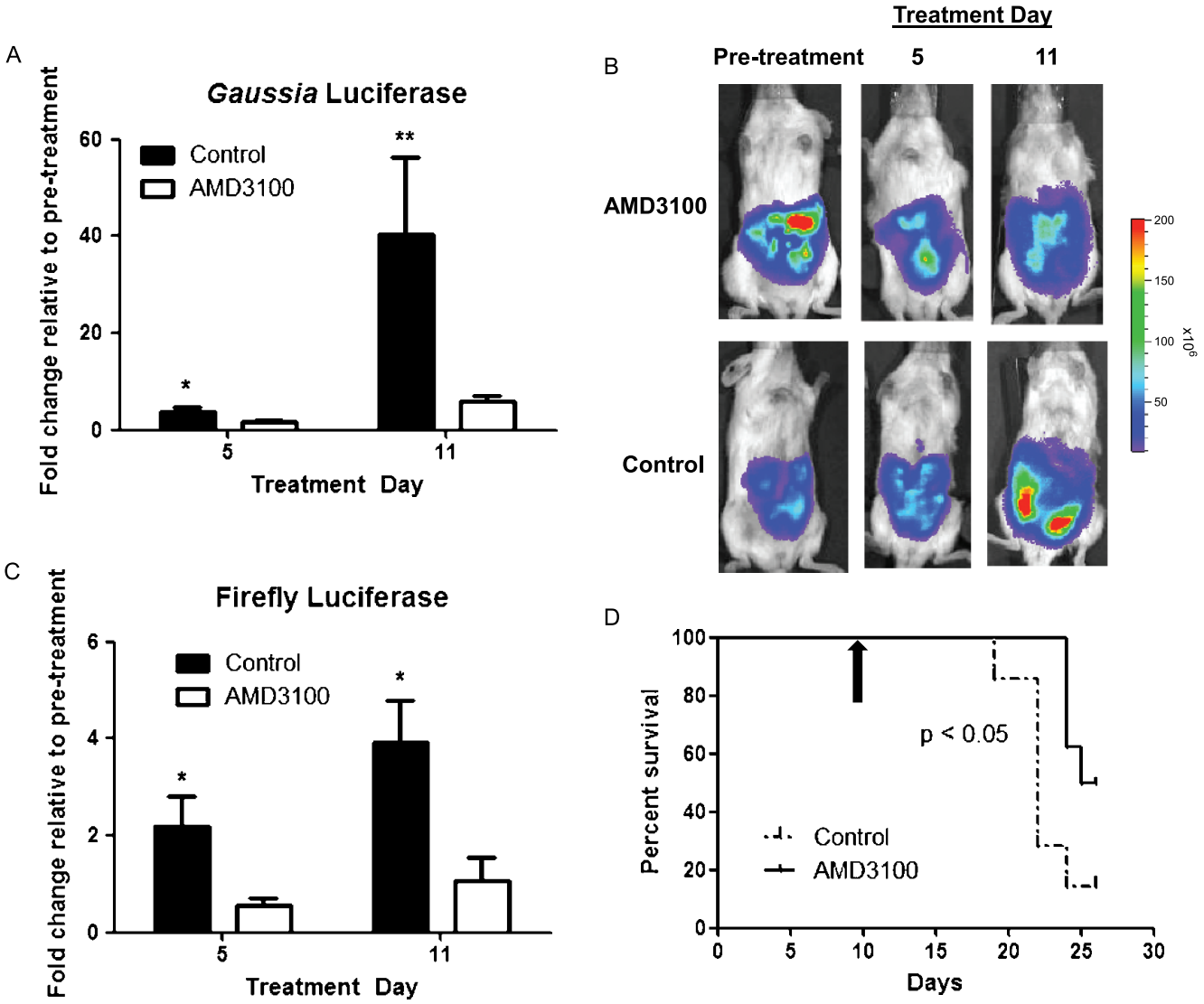

Figure 6. AMD3100 reduces tumor growth and prolongs survival of mice with metastatic ovarian cancer. (A) Mice were injected intraperitoneally with 1.25×10^5 cells each of HeyA8-CXCL12-CG and NG-CXCR4 cells. After 10 days of tumor growth, mice were imaged for baseline *Gaussia* luciferase activity immediately before implantation of osmotic infusion pumps with AMD3100 or vehicle control. Repeat imaging studies for *Gaussia* luciferase complementation were performed on days 5 and 11 of treatment. The fold change in *Gaussia* luciferase bioluminescence relative to the pretreatment baseline value was determined for each mouse, and mean values for each group ± SEM were graphed. (B) Representative firefly luciferase images for relative numbers of HeyA8-NG-CXCR4 cells before and on days 5 and 11 of treatment with AMD3100 or vehicle control. Scale bar shows pseudocolor display for photon flux values on all images. (C) Quantified data for tumor growth measured by firefly luciferase activity. Fold change in bioluminescence on days 5 and 11 of treatment was determined relative to pretreatment values for each mouse, and data were presented as mean values ± SEM ($n = 8$ per group). (D) Kaplan-Meier survival curve for mice treated with AMD3100 or vehicle control. Black arrow denotes start of therapy. *$P < .05$. **$P < .01$.

targeting CXCL12-CXCR4 may offer therapeutic benefits in advanced ovarian cancer.

Similar to our current research, a previous study by Kajiyama et al. [32] showed that AMD3100 limited tumor dissemination and overall tumor burden in a mouse model of intraperitoneal ovarian cancer. However, the previous study reported no effect of AMD3100 treatment on overall survival. This disparity may be due to the use of different cell lines and/or nude mice *versus* the more immunocompromised mouse strain we used. In addition, Kajiyama et al. injected AMD3100 intraperitoneally for treatment studies, whereas we used subcutaneous osmotic infusion pumps to deliver constant levels of this drug. Chemotherapy for ovarian cancer typically is administered intraperitoneally, but AMD3100 is cleared rapidly *in vivo* [33,34]. Whereas *Gaussia* luciferase complementation established that intraperitoneal delivery of AMD3100 can block CXCL12-CXCR4, we used osmotic infusion pumps to achieve sustained inhibition of ligand-receptor binding and maximize the ability to identify a survival benefit. CXCL12-CXCR4 inhibitors with improved pharmacokinetics will mitigate this problem. During the preparation of this article, Righi et al. [35] also demonstrated that AMD3100 delivered from an osmotic infusion pump reduced growth of ovarian cancer cells and extended survival in an immunocompetent mouse model. Collectively, these studies establish CXCL12-CXCR4 as a promising molecular target for ovarian cancer therapy and emphasize the

importance of imaging technologies to monitor effective inhibition of this pathway *in vivo*.

The combination of *Gaussia* luciferase complementation reporters for CXCL12-CXCR4 binding and firefly luciferase for tumor progression offers notable advantages for discovery and development of new agents targeting this ligand-receptor pair. The HeyA8 ovarian cancer cells can be used to quantify ligand-receptor binding in cell-based, multiwell plate assays compatible with high-throughput screening. These same reporter cells can then be used to test promising lead compounds in preclinical animal models of ovarian cancer. The complementation system provides the unique capability to quantify pharmacodynamics of therapeutic compounds at the target site rather than relying on serum levels of compound or inferring receptor inhibition in surrogate tissues. Inhibition of the target pathway then can be correlated directly with effects on tumor growth in preclinical models. Because the reporter constructs all are in lentiviral vectors, the imaging reporters could be introduced readily into other cell lines and primary ovarian cancer cells, establishing a panel of reporter cell types for cell-based assays and animal models. A limitation of the existing HeyA8 reporter cells is that CXCL12-CG and NG-CXCR4 were expressed by separate populations of cells, necessitating coculture or coimplantation of two different cell types. We tried coexpressing both reporters in the same cell, but the magnitude of signal from CXCL12-CG binding to NG-CXCR4 was notably lower (Luker KE, et al., unpublished data). We are working to overcome this limitation.

In the current study, we analyzed effects of AMD3100 on mice with established intraperitoneal ovarian cancer metastases. Although this model reproduces the stage at which most patients present with ovarian cancer, it bypasses steps of metastasis including invasion and dissemination of malignant cells from the ovary and/or fallopian tube into the peritoneum. Because cell culture studies demonstrate that CXCL12-CXCR4 signaling promotes these processes, inhibitors of this signaling pathway also may limit progression from localized disease. Further testing with genetically engineered mouse models of ovarian cancer or intraovarian injection of malignant cells will be required to validate this hypothesis. We administered AMD3100 as a single therapeutic agent because of the challenges of managing toxicities in mice treated with multiple compounds. In clinical practice, CXCL12-CXCR4 inhibitors would almost certainly be used as part of integrated therapy for ovarian cancer, including debulking surgery and combination chemotherapy. Our findings support further development of CXCL12-CXCR4 inhibitors for therapy for ovarian cancer and other malignancies and translation of such agents to clinical trials in ovarian cancer.

Acknowledgments

The authors thank ChemoCentryx for small molecule inhibitors of CXCR7.

References

[1] Bast RJ, Hennessy B, and Mills G (2009). The biology of ovarian cancer: new opportunities for translation. *Nat Rev Cancer* **9**, 415–428.

[2] Rattan R, Graham R, Maguire J, Giri S, and Shridhar V (2011). Metformin suppresses ovarian cancer growth and metastasis with enhancement of cisplatin cytotoxicity *in vivo*. *Neoplasia* **13**, 483–491.

[3] Zillhardt M, Christensen J, and Lengyel E (2010). An orally available small-molecule inhibitor of c-Met, PF-2341066, reduces tumor burden and metastasis in a preclinical model of ovarian cancer metastasis. *Neoplasia* **12**, 1–10.

[4] Kim S, Kim J, Kim S, Brantley E, Yun S, He J, Maya M, Zhang F, Wu Q, Lehembre F, et al. (2011). Macitentan (ACT-064992), a tissue-targeting endothelin receptor antagonist, enhances therapeutic efficacy of paclitaxel by modulating survival pathways in orthotopic models of metastatic human ovarian cancer. *Neoplasia* **13**, 167–179.

[5] Wang H, Zhou M, Shi B, Zhang Q, Jiang H, Sun Y, Liu J, Zhou K, Yao M, Gu J, et al. (2011). Identification of an exon 4–deletion variant of epidermal growth factor receptor with increased metastasis-promoting capacity. *Neoplasia* **13**, 461–471.

[6] Barbieri F, Bajetto A, and Florio T (2010). Role of chemokine network in the development and progression of ovarian cancer: a potential novel pharmacological target. *J Oncol* **2010**, 426956.

[7] Jiang Y, Wu X, Shi B, Wu W, and Yin G (2006). Expression of chemokine CXCL12 and its receptor CXCR4 in human epithelial ovarian cancer: an independent prognostic factor for tumor progression. *Gynecol Oncol* **103**, 226–233.

[8] Scotton C, Wilson J, Milliken D, Stamp G, and Balkwill F (2001). Epithelial cancer cell migration: a role for chemokine receptors? *Cancer Res* **61**, 3.

[9] Foussat A, Balabanian K, Amara A, Bochet-Delbos L, Durand-Gasselin I, Baleux F, Couderc J, Galanaud P, and Emilie D (2001). Production of stromal cell–derived factor 1 by mesothelial cells and effects of this chemokine on peritoneal B lymphocytes. *Eur J Immunol* **31**, 350–359.

[10] Scotton C, Wilson J, Scott K, Stamp G, Wilbanks G, Fricker S, Bridger G, and Balkwill F (2002). Multiple actions of the chemokine CXCL12 on epithelial tumor cells in human ovarian cancer. *Cancer Res* **62**, 5930–5938.

[11] Yuecheng Y and Xiaoyan X (2007). Stromal-cell derived factor-1 regulates epithelial ovarian cancer cell invasion by activating matrix metalloproteinase-9 and matrix metalloproteinase-2. *Eur J Cancer Prev* **16**, 430–435.

[12] Miyanishi N, Suzuki Y, Simizu S, Kuwabara Y, Banno K, and Umezawa K (2010). Involvement of autocrine CXCL12/CXCR4 system in the regulation of ovarian carcinoma cell invasion. *Biochem Biophys Res Commun* **403**, 154–159.

[13] Kryczek I, Lange A, Mottram P, Alvarez X, Cheng P, Hogan M, Moons L, Wei S, Zhou L, Machelon V, et al. (2005). CXCL12 and vascular endothelial growth factor synergistically induce neoangiogenesis in human ovarian cancers. *Cancer Res* **65**, 465–472.

[14] Orimo A, Gupta P, Sgroi D, Arenzana-Seisdedos F, Delaunay T, Naeem R, Carey V, Richardson A, and Weinberg R (2005). Stromal fibroblasts present in invasive human breast carcinomas promote tumor growth and angiogenesis through elevated SDF-1/CXCL12 secretion. *Cell* **121**, 335–348.

[15] Kollmar O, Rupertus K, Scheuer C, Junker B, Tilton B, Schilling M, and Menger M (2007). Stromal cell–derived factor-1 promotes cell migration and tumor growth of colorectal metastasis. *Neoplasia* **9**, 862–870.

[16] Luker K, Gupta M, and Luker G (2008). Imaging CXCR4 signaling with firefly luciferase complementation. *Anal Chem* **80**, 5565–5573.

[17] Luker K, Gupta M, Steele J, Foerster B, and Luker G (2009). Imaging ligand-dependent activation of CXCR7. *Neoplasia* **11**, 1022–1035.

[18] Luker K, Mihalko L, Schmidt B, Lewin S, Ray P, Shcherbo D, Chudakov D, and Luker G (2011). *In vivo* imaging of ligand receptor binding with *Gaussia* luciferase complementation. *Nat Med*, E-pub ahead of print December 4.

[19] Shcherbo D, Shemiakina I, Ryabova A, Luker K, Schmidt B, Souslova E, Gorodnicheva T, Strukova L, Shidlovskiy K, Britanova O, et al. (2010). Near infrared fluorescent proteins. *Nat Methods* **7**, 827–829.

[20] Luker K, Steele J, Mihalko L, and Luker G (2010). Constitutive and chemokine-dependent internalization and recycling of CXCR7 in breast cancer cells to degrade chemokine ligands. *Oncogene* **29**, 4599–4610.

[21] Luker K, Gupta M, and Luker G (2009). Bioluminescent CXCL12 fusion protein for cellular studies of CXCR4 and CXCR7. *Biotechniques* **47**, 625–632.

[22] Luker K, Gupta M, and Luker G (2009). Imaging chemokine receptor dimerization with firefly luciferase complementation. *FASEB J* **23**, 823–834.

[23] Tannous B, Kim D, Fernandez J, Weissleder R, and Breakefield X (2005). Codon-optimized *Gaussia* luciferase cDNA for mammalian gene expression in culture and *in vivo*. *Mol Ther* **11**, 435–443.

[24] Smith M, Luker K, Garbow J, Prior J, Jackson E, Piwnica-Worms D, and Luker G (2004). CXCR4 regulates growth of both primary and metastatic breast cancer. *Cancer Res* **64**, 8604–8612.

[25] Barbolina M, Kim M, Liu Y, Shepard J, Belmadani A, Miller R, Shea L, and Stack M (2010). Microenvironmental regulation of chemokine (C-X-C-motif) receptor 4 in ovarian carcinoma. *Mol Cancer Res* **8**, 653–664.

[26] Remy I and Michnick S (2006). A highly sensitive protein-protein interaction assay based on *Gaussia* luciferase. *Nat Methods* **3**, 977–979.

[27] De Clercq E (2003). The bicyclam AMD3100 story. *Nat Rev Drug Discov* **2**, 581–587.

[28] Zabel B, Wang Y, Lewen S, Berahovich R, Penfold M, Zhang P, Powers J, Summers B, Miao Z, Zhao N, et al. (2009). Elucidation of CXCR7-mediated

signaling events and inhibition of CXCR4-mediated tumor cell transendothelial migration by CXCR7 ligands. *J Immunol* **183**, 3204–3211.

[29] Zhang W, Navenot J, Haribabu B, Tamamura H, Hiramatu K, Omagari A, Pei G, Manfredi J, Fujii N, Broach J, et al. (2002). A point mutation that confers constitutive activity to CXCR4 reveals that T140 is an inverse agonist and that AMD3100 and ALX40-4C are weak partial agonists. *J Biol Chem* **277**, 24515–24521.

[30] Yasumoto K, Koizumi K, Kawashima A, Saitoh Y, Arita Y, Shinohara K, Minami T, Nakayama T, Sakurai H, Takahashi Y, et al. (2006). Role of the CXCL12/CXCR4 axis in peritoneal carcinomatosis of gastric cancer. *Cancer Res* **66**, 2181–2187.

[31] Kulbe H, Hagemann T, Szlosarek P, Balkwill F, and Wilson J (2005). The inflammatory cytokine tumor necrosis factor-α regulates chemokine receptor expression on ovarian cancer cells. *Cancer Res* **65**, 10355–10362.

[32] Kajiyama H, Shibata K, Terauchi M, Ino K, Nawa A, and Kikkawa F (2008). Involvement of SDF-1α/CXCR4 axis in the enhanced peritoneal metastasis of epithelial ovarian carcinoma. *Int J Cancer* **122**, 91–99.

[33] Armstrong D, Bundy B, Wenzel L, Huang H, Baergen R, Lele S, Copeland L, Walker J, Burger R, and Group GO (2006). Intraperitoneal cisplatin and paclitaxel in ovarian cancer. *N Engl J Med* **354**, 34–43.

[34] Hendrix C, Flexner C, MacFarland R, Giandomenico C, Fuchs E, Redpath E, Bridger G, and Henson G (2000). Pharmacokinetics and safety of AMD-3100, a novel antagonist of the CXCR-4 chemokine receptor, in human volunteers. *Antimicrob Agents Chemother* **44**, 1667–1673.

[35] Righi E, Kashiwagi S, Yuan J, Santosuosso M, Leblanc P, Ingraham R, Forbes B, Edelblute B, Collette B, Xing D, et al. (2011). CXCL12/CXCR4 blockade induces multimodal antitumor effects that prolong survival in an immunocompetent mouse model of ovarian cancer. *Cancer Res* **71**, 5522–5534.

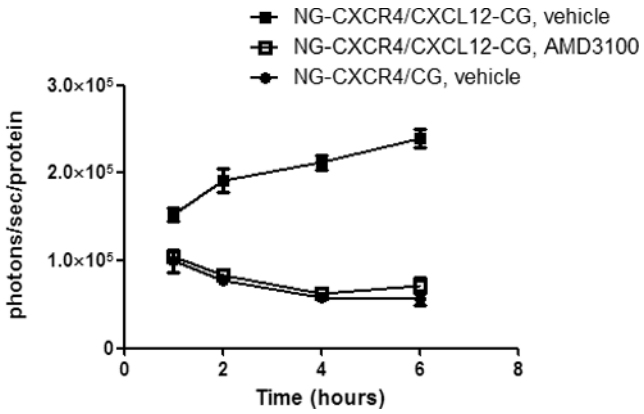

Figure W1. Cocultures of HeyA8-CXCL12-CG/NG-CXCR4 cells were treated for increasing periods through 6 hours with 1 μM AMD3100 or matched volume of PBS vehicle control. Parallel cocultures of HeyA8-CG/NG-CXCR4 cells were incubated with PBS vehicle control for the same periods. Photons from *Gaussia* luciferase bioluminescence were quantified and normalized to total protein per well. Data were presented as mean values ± SEM (n = 4 per condition).

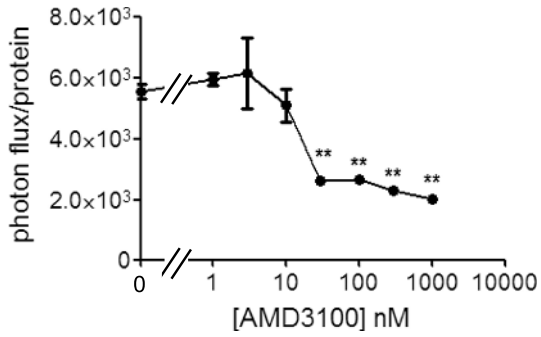

Figure W3. HeyA8-CXCL12-CG and NG-CXCR4 cells were recovered from ascites of mice treated with AMD3100. Mixtures of cells recovered from mice were treated for 2 hours with increasing concentrations of AMD3100 before quantifying bioluminescence from *Gaussia* luciferase complementation (n = 4 per condition). Data were normalized to relative amounts of total protein per well and graphed as mean values ± SEM. $^{**}P < .01$.

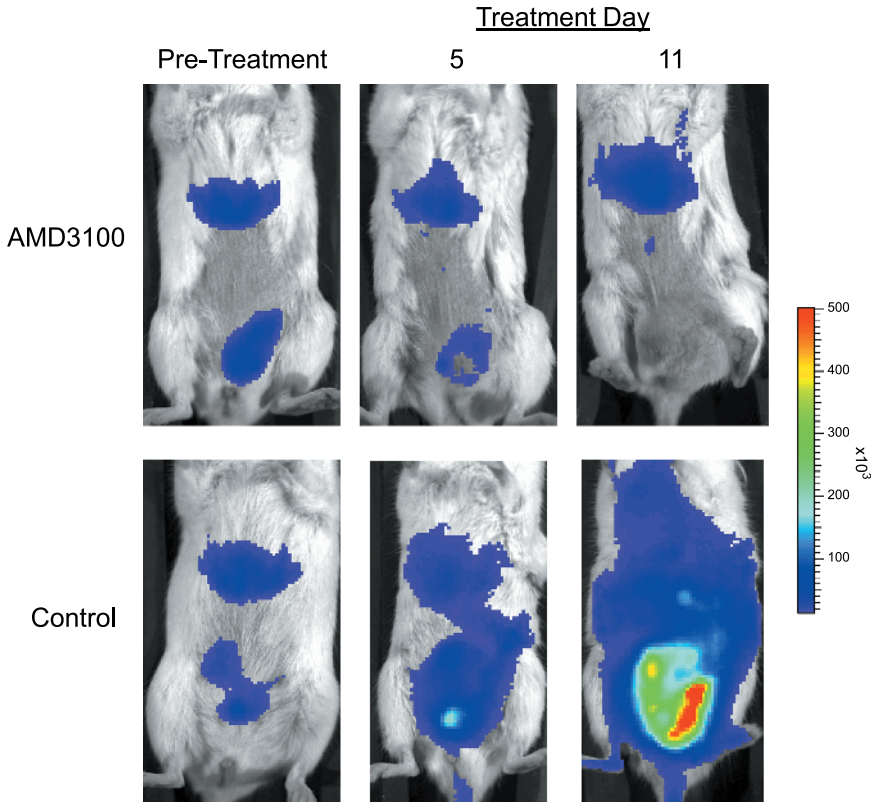

Figure W2. Representative bioluminescence images for *Gaussia* luciferase complementation between CXCL12-CG and NG-CXCR4 in mice are shown before (pretreatment) and during treatment with AMD3100 or vehicle control. Images were obtained on days 5 and 11 of treatment. Scale bar denotes range of pseudocolors used to depict photon flux for all images.